(54) Title: TRANSTHORACIC PULMONARY DOPPLER ULTRASOUND

FIG. 1

(57) Abstract: Operation of a patient's heart or lungs may be analyzed by transmitting ultrasound energy into the patient's lung, and detecting Doppler shifts of reflected ultrasound induced by moving borders between blood vessels in the lung and air filled alveoli that surround the blood vessels. Movement of the border is caused by pressure waves in the blood vessels that result in changes in diameter of those blood vessels. The detected Doppler shifts are processed with an algorithm designed to increase signal from the moving border with respect to other reflected ultrasound signals and the results are then displayed.

TRANSTHORACIC PULMONARY DOPPLER ULTRASOUND

CROSS REFERENCE TO RELATED APPLICATIONS

[0001]   This Application claims the benefit of US Provisional Application 61/255,322, filed October 27, 2009, US Provisional Application 61/326,133, filed April 20, 2010, and US Provisional Application 61/405,454, filed October 21, 2010, each of which is incorporated herein by reference.

BACKGROUND

[0002]   The use of ultrasound Doppler for Spectral measurement of blood flow velocity in arteries and veins is well established. One widely used procedures for making such measurements is based on three typical stages: an initial identification of the target area (where flow is to be measured) using ultrasound imaging; placement of a marker on the appropriate position on the image; and switching the echo device from Imaging mode to Spectral Doppler Examination mode in order to display the flow velocities in real-time. This procedure can be used, for example, to measure the blood flow in a pulmonary vein.

[0003]   Another procedure, which is relatively new, is used for Trans Cranial Doppler (TCD) measurements, as well as some peripheral vascular studies. In this procedure the ultrasound beam is directly aimed at the known location of the target, without relying on imaging. As the structure and positioning of the human skull and its constituents are relatively fixed and known, specific vessels such as the arteries of the circle of Willis, at the base of the brain, are being studied in this procedure by echo Doppler alone (i.e. without imaging). The fact that the flow velocity measurements can be made without imaging enables one to do the measurements through the bones of the skull that attenuate and scatter the ultrasound beam to such an extent that practical images cannot be obtained.

2

[0004]   While trans-cranial Doppler measurements are now in routine use to study

structures in the brain, applying this technology trans-thoracically monitor pulmonary vessels

was heretofore considered impossible. This is due to the fact that the lungs contain numerous

air pockets that attenuate and scatter ultrasound far more than bone. In view of this, except

for the initial, large, segments of the pulmonary vessels that are not masked by lung tissue,

arterial and venous flow velocity in the pulmonary vasculature and the lung tissue itself have

not been studied by Doppler ultrasound.

SUMMARY

[0005]   One aspect of the invention is directed to a method of evaluating the

functionality of a patient's heart or lungs. This method includes the steps of transmitting

ultrasound energy into the patient's lung and detecting Doppler shifts of reflected ultrasound

induced by moving borders between blood vessels in the lung and air filled alveoli that

surround the blood vessels. Movement of the border is caused by pressure waves in the

blood vessels that result in changes in diameter of those blood vessels. The detected Doppler

shifts are processed with an algorithm designed to increase signal from the moving border

with respect to other reflected ultrasound signals and to output the processed power and

velocity data which is then displayed.

[0006]   Another aspect of the invention is directed to a method of evaluating the

functionality of a patient's heart or lungs. This method includes the steps of obtaining, using

an ultrasound probe that is aimed at the patient's lung, Doppler ultrasound power and

velocity data for a period of time that corresponds to at least one cardiac cycle. The power

and velocity data obtained in the obtaining step are processed using at least one noise

reduction algorithm, and the processed power and velocity data are displayed. An

abnormality in at least one of (a) a feature on the display that corresponds to systolic

ventricular contraction, (b) a feature on the display that corresponds to ventricular relaxation, (c) a feature on the display that corresponds to a diastolic rapid filling phase, (d) a feature on the display that corresponds to diastasis, and (e) a feature on the display that corresponds to atrial contraction is correlated with an abnormal condition of the patient's heart or lungs.

[0007]   Another aspect of the invention is directed to a method of evaluating the functionality of a patient's heart or lungs. This method includes the steps of obtaining, using an ultrasound probe that is aimed at the patient's lung, Doppler ultrasound power and velocity data for a period of time that corresponds to at least one cardiac cycle. The power and velocity data obtained in the obtaining step are processed using at least one noise reduction algorithm. After processing, the results are checked for abnormalities in (a) a feature of the processed power and velocity data that corresponds to systolic ventricular contraction, (b) a feature of the processed power and velocity data that corresponds to ventricular relaxation, (c) a feature of the processed power and velocity data that corresponds to a diastolic rapid filling phase, (d) a feature of the processed power and velocity data that corresponds to diastasis, and (e) a feature of the processed power and velocity data that corresponds to atrial contraction. An absence of abnormalities is correlated with a normal condition of the patient's heart or lungs.

[0008]   Another aspect of the invention is directed to a method of evaluating the functionality of a patient's heart or lungs. This method includes the steps of obtaining, using an ultrasound probe that is aimed at a first position of the patient's lungs, a first set of Doppler ultrasound power and velocity data for a period of time that corresponds to at least one cardiac cycle and obtaining, using an ultrasound probe that is aimed at a second position of the patient's lungs, a second set of Doppler ultrasound power and velocity data for a period of time that corresponds to the at least one cardiac cycle. A first output is generated by

processing the first set of data using at least one noise reduction algorithm, and a second

output is generated by processing the second set of data using at least one noise reduction

algorithm.

BRIEF DESCRIPTION OF THE DRAWINGS

[0009]   FIG. 1 is a block diagram of an embodiment of a Transthoracic Pulmonary

Doppler ("TPD") System.

[0010]   FIG. 2 depicts an example of an output generated by the system of FIG. 1.

[0011]   FIG. 3 is a schematically illustration of five features in the output shown in

FIG. 2.

[0012]   FIG. 4A depicts the "classical Model" of clinical Doppler measurements.

[0013]   FIG. 4B depicts the origin of the Doppler signals picked up using TPD.

[0014]   FIG. 5A compares a TPD output of a normal subject with tracings of blood

flow velocity in a pulmonary artery and vein.

[0015]   FIGS. 5B-E are TPD outputs for normal breathing and during various

respiratory maneuvers.

[0016]   FIG. 6 depicts a TPD output averaged over ten cardiac cycles from a normal

subject.

[0017]   FIG. 7A depicts a TPD output for a normal sinus rhythm followed by a

propagating atrial extra-systole.

[0018]   FIG. 7B depicts a TPD output when an atrial non-propagating extra-systole is present.

[0019]   FIG. 8 depicts a TPD output when extra-systolic contractions are present.

[0020]   FIG. 9 depicts a TPD output when atrial fibrillation occurs.

[0021]   FIGS. 10A-C depict experimental data on the average peak positive and negative velocities for three features of a TPD output.

[0022]   FIGS. 11A is a graphical representation of the velocity differences between normal and abnormal subjects.

[0023]   FIG. 11B is a graphical representation of power differences between normal, COPD, and fibrosis subjects.

[0024]   FIG. 12 depicts the boundaries between features determined by an automatic feature recognition algorithm.

DESCRIPTION OF THE PREFERRED EMBODIMENTS

[0025]   The inventors have recognized that the pulmonary circulation and the pulmonary light scattering properties may be significantly modified in a large variety of cardio-pulmonary patho-physiological conditions and diseases, and that such information may be of significant diagnostic and therapeutic importance. The embodiments described herein are designed to monitor the functionality of the arteries and veins in the lungs, as well as the integrity and functionality of the lung tissues that surround them, using Doppler ultrasound. It is referred to herein as "Transthoracic Pulmonary Doppler" or "TPD".

[0026]   FIG. 1 is a block diagram of one such embodiment. A Doppler ultrasound

machine 12 in conjunction with the probe 11 (which includes an ultrasound transducer) is

used to determine the power at every relevant velocity in a target region of the subject 10,

over time, in a conventional manner. This may be accomplished by generating pulsed

ultrasound beams, picking up the reflected energy, calculating the Doppler shifts, and

processing the data thus obtained to provide the matrix of power and corresponding velocities

of the ultrasound reflectors. One example of a suitable Doppler ultrasound machine 12 is the

Sonara/tek pulsed Trans-Cranial-Doppler device (available from Viasys, Madison,

Wisconsin, US), which is a pulsed Doppler system. The Doppler ultrasound machine 12

sends the data that it captures to a personal computer 13 that is loaded with software to

generate a conventional Doppler ultrasound display (e.g., on a monitor associated with the

computer 13) in which the x axis represents time, the y axis represents velocity, and power is

represented by color. Suitable software for controlling the ultrasound parameters is also

available from Viasys. Note that in alternative embodiments, the functions of the Doppler

ultrasound machine 12 and personal computer 13 may be combined into a single device.

[0027]   Preferably, an ECG system 14 is also provided. The ECG system 14

interfaces with conventional ECG leads 15 and generates an output in any conventional

manner. The output is preferably synchronized in time with the Doppler ultrasound machine

12 so that both an ECG and ultrasound display can be displayed on the same time scale. The

output of the ECG system 14 is provided to the personal computer 13 in any conventional

manner. In alternative embodiments, it may be combined by the Doppler ultrasound machine

12 instead.

[0028]   A standard TCD probe such as a 21 mm diameter, 2 MHz sensor with a focal

length of 4 cm may be used as the probe 11. Suitable probes are available from Viasys for

use with their Sonara/tek machines. Conventional probes for making Doppler ultrasound

measurements of peripheral or cardiac blood vessels may also be used. These applications,

however, typically use narrow beams, often shaped using a phased array transducer, to

provide a high spatial resolution that is helpful for making geometrical characterization of the

relatively small targets. While these narrow beams can produce usable results in the context

of TPD, some preferred alternative embodiments use relatively wide beams, for example

beams with an effective cross section of at least ½ cm (e.g., between ½ and 3 cm). This may

be accomplished by using a smaller transducer, and by using single element transducers

instead of phased array transducers that are popular in other anatomical applications. When a

wider beam is used, the system can take advantage of the fact that the lungs contain relatively

large complexes of unspecified geometrical shape consisting of blood vessels (both arteries

and veins) and their surrounding lung tissues.

[0029]   Note that since imaging the lung with ultrasound is impossible because of the

scattering, one has to scan for targets without guidelines, except for the known anatomy.

Note also that scattering lowers the advantage of scanning by either phase array or by

mechanical means. Furthermore, since the whole lung depth induces scattering, CW

(continuous wave) ultrasound is less effective than PW (pulsed wave) Doppler ultrasound for

pulmonary applications. Therefore, some preferred embodiments utilize PW ultrasound with

relatively wide beams. Optionally, such embodiments may employ multiple sensors

positioned on the surface of the body.

[0030]   Optionally, specially selected or designed ultrasound probes and/or suitable

beam power control may be used, including dynamic adjustable beam shape and size so as to

enable measurement from variable tissue volumes. Note that in contrast to when Doppler is

8

used for other tissue targets, here the average and integral of signals originating from relatively large volumes contain valuable information.

[0031]   In addition to the standard software for generating a display from the Doppler signals, the personal computer 13 preferably includes software for activating the TPD and selecting the desired operating mode, display mode, and storage modes. The personal computer 13 also includes or has access to appropriate data storage resources (e.g., local or remote hard drives). The personal computer 13 preferably processes the original velocity-and-power vs. time data using one or more noise reduction (NR) algorithms that are optimized to minimize the noise created by the signal scattering and attenuation by the lung tissue.

[0032]   One preferred approach to noise reduction involves two phases – averaging and edge detection. In the first phase, an averaged signal from a number of cardiac cycles is obtained by averaging the power/velocity data of N characteristic signals, where each of the N signals preferably represents a single cardiac cycle. N is preferably an integer between 4 and 20 (e.g., 10). Preferably, each signal is bounded by an R-wave at each end, although in alternative embodiments other points on the cardiac cycle may be used as a time reference point. The calculated averaged signal is assumed to characterize the spectrogram behavior for the subject, and therefore is the basis on which the relevant features are later determined. Note that while it is preferable to perform this averaging phase, in alternative embodiments this phase could be skipped and subsequent processing could be performed on data from a single cardiac cycle.

[0033]   The second phase is edge detection and envelope calculation. In this phase, we delineate, in regards to both amplitude and time, the power and velocity signal tracings vs.

time, and thereby separate the sections that represent the blood vessel movement (i.e., the signal) from the noise. One or more noise reducing algorithms may be used during this phase. In one preferred embodiment, two specific edge detection algorithms, referred to herein as algorithm A and algorithm B, are applied to the data. Both algorithm A and algorithm B are applied on the averaged signal and calculate the edge (i.e., envelope) between the signal and the noise in the averaged image.

[0034]   Algorithm A is a local, one-dimensional method in which the edge (e_A) between signal and noise at a given time is defined according to the statistics of the data at the proximity of this time only. This algorithm includes two steps: In the first step, we define, at any given time (ti), a threshold 'thr(ti)' for each power spectrum A(ti) by searching for a region of lowest energy in the proximity of ti. We then set thr(ti) to be equal to the highest power level in this region. Next, we apply thr(ti) on A(ti) and deem all parts of A(ti) above thr(ti) as corresponding to movement regions and all other parts as corresponding to noise.

[0035]   In the second step of Algorithm A, we refine the initial distinction between flow and noise by using the statistics of noise: In this step, we assume down estimation (flow being included in noise region); adjust envelopes detection to exclude flow pixels from noise regions; and identify pixels of flow in noise regions by their relatively high values. Symbolically, this can be represented by the following three steps:

(a) For each t = {1,2, ... N}, calculate P(t) = {mean of A(t) in noise region}

(b) Define a threshold 'thr2' which is based on the average and std of {P(1),P(2), ... P(N)}

(c) For each t' where P(t')>thr2, reduce P(t') by raising upper envelope or lowering the lower envelope until P(t')<=thr2.

For better results, steps (a)-(c) are preferably repeated a number of time (e.g., 10 times).

[0036]   Algorithm B is an edge detection algorithm that treats the data as two-dimensional image. In this method, the signal is seen as an object surrounded by noise which is segmented out of it, and the edge (e_B) is calculated accordingly. This segmentation method is an implementation of the Chan-Vese algorithm. (See Chan T.F., Vese L.A., Active contours without edges. Image Processing IEEE, Transactions on, Volume 10, Issue 2: 266-277 (Feb 2001), which is incorporated herein by reference).

[0037]   The edge calculated by Algorithm A ($e_A=[e_A(t1),e_A(t2),...]$) is then combined with the edge calculated by Algorithm B ($e_B=[e_B(t1),e_B(t2),...]$). One suitable approach to combining those two edges is by assuming that the desired edge passes between the two edges that were found. This may be done using a variety of approaches. One approach is take a simple average of the results from algorithm A and algorithm B at each point. Another approach for combining those two edges is to create an array of weights ($w=[w(t1),w(t2),...]$) as follows: (1) the power levels of the image at the gap are integrated along time; (2) the result is linearly transformed to have a maximal value of '1' and minimal value of '0'; and (3) the output for the edge at a time point ti is then defined by the following equation: $e(ti) = w(ti)*e_A(ti)+(1-w(ti))*e_B(ti)$.

[0038]   The resulting output is preferably smoothened via a one-dimensional median filter (e.g., of order 3) and displayed, and FIG. 2 depicts an example of the resulting output. Note that in alternative embodiments, only one algorithm (i.e., either algorithm A or algorithm B or a different NR algorithm) may be used, either taken alone or combined with other NR algorithms.

[0039]   FIG. 2 depicts the velocities 22 of the ultrasound reflectors in the right lung of a normal subject obtained using a 2 MHz Doppler ultrasound system with the probe

11

positioned about 3 cm to the right of the sternum and 7 cm up from the level of the tip of the

xiphoid bone (about the 4th intercostal space). The ultrasound beam was roughly normal to

the chest surface. In FIG. 2, darker regions correspond to higher powers. A conventional

ECG 24 is preferably also displayed on the bottom of FIG. 2. Similar recordings were

obtained from recordings at depths (gates) of up to 14 cm and from the left lung in areas not

dominated by the heart. Maximal signal strength over the right lung was recorded at a depth

of 8 – 9 cm below the surface.

[0040]   The same pulse repetition frequency (PRF) that is used in conventional TCD

systems (i.e., 3-10 kHz) may be used for TPD systems. However, TPD sonograms 22

includes of a number of medium velocity signals that have the same periodicity as the cardiac

cycle and usually reach values only up to about 30 cm/sec. Due to these relatively low peak

velocities (as compared to Doppler flow measurements in large arteries), the TPD PRF used

may be set to a value that is lower than standard pulsed Doppler systems. By lowering the

PRF to 1-2 kHz, the effective beam penetration depth is at least doubled as compared with

the conventional PRF. This is important as ultrasound velocity in the lung is about 30-50%

lower than in fat, muscle etc. thus lowering the effective penetration depth. Preferably, the

software is configured to take this lower velocity into account. The transition point where the

signals originating in the lung can be detected by recognizing the shallowest point at which

the lung signals (i.e., signals with very large returns) appear. Note that measurements from

different lung depth result in very similar tracings, and that the traces for other apparently

normal subjects had generally similar characteristics.

[0041]   It is seen that, at each polarity (positive or negative), one can usually identify

five significant features with relatively high energy and a roughly triangular shape. These

five features are schematically illustrated and numbered #1-5 in FIG. 3. Each of these

features includes a positive component (i.e., positive velocities, indicating that the flow

direction is towards the probe) and a corresponding negative component (i.e., negative

velocities, indicating that the flow direction is away from the probe), with a high degree of

positive/negative symmetry. Thus, each of these features indicates simultaneous movements

in opposite directions. As seen in FIG. 3, these features are synchronous with the cardiac

cycle (note the R waves 26 in the ECG 24).

[0042]   THEORY OF OPERATION

[0043]   The above described signals recorded over the lungs appear to have a unique

origin. As is well known the lungs consist of a very large number of alveolar ducts, alveolar

sacs and alveoli which can be regarded as miniature gas volumes encapsulated by a very thin

membrane. The alveoli, which can be assumed to be reasonably represented by spheroids,

have dimensions in the range of 50-150 μ. When exposed to ultrasound waves these natural

lung components resemble in many respects ultrasound contrast media used in sonography.

(Ultrasound contrast agents are gas-filled microbubbles with a high degree of echogenicity,

i.e., the ability of an object to reflect the ultrasound waves.) The echogenicity difference

between the alveoli and soft tissues is very large and therefore most of the energy is reflected.

[0044]   Although scattering makes it impossible to obtain ultrasound images of lung

structures, it is actually helpful in detecting movement of the highly reflective border between

soft tissue and alveoli. Movements of this border are induced by respiration and even more

so by cardiac contraction and mechanical pulse waves travelling in the blood and the

pulmonary blood vessels. It is well known that the pulmonary blood vessels have a very high

compliance (i.e., much larger than that of the systemic circulation), and the air filled alveolar

tissue surrounding the vessels is highly compressible. Thus, pressure waves in the pulmonary

arteries and veins result in significant changes in their diameter. These changes in turn move

the highly reflective border, compressing and moving the alveoli, alveolar sacs, etc. in their

vicinity. As the ultrasound propagation velocity in tissue and air are very different, there is a

mechanical coupling mismatch at their border resulting in high echogenicity and strong

ultrasound reflections, which in this case is from a moving reflector that results in Doppler

shifts. These reflections are often on the order of 100 dB above the noise level (in

comparison to typical intensities measured from blood flowing in arteries, which are in the

range of 30-40 dB above noise level). Because these signals are so strong, the returns are

picked up by the Doppler system even though they may be partially masked by a layer of

stationary lung tissue, which attenuates ultrasound energy by about 40 dB/cm.

[0045]   FIGS. 4A and FIG. 4B illustrate the differences between conventional Doppler

signals and the signals picked up by TPD through the chest wall. FIG. 4A illustrates the

"classical Model" of clinical Doppler measurements in which the device measures the

Doppler frequency shift resulting from blood flow 42 in arteries and veins, or more

specifically from the movement of the erythrocytes 43 (which reflect the ultrasound waves)

through those vessels 44.

[0046]   FIG. 4B illustrates the origin of the Doppler signals picked up using TPD.

Here the changes in pressure induce changes in vessel diameter because as the heartbeat

generates pressure pulses that urges the blood 32 through the vessel, the vessel walls 34

momentarily bulge outwards and compress the air filled alveoli, alveolar sacs, etc. 35 that

surround them. The Doppler shifts of the reflected ultrasound induced by the moving vessel

– alveoli border are translated to power-and-velocity vs. time plots and displayed by the TPD

system. It is expected that the majority of these signals are generated by small and

intermediate size arteries and veins. A unique feature of signals generated in this mode (as

opposed to those generated by the flow of blood in the rest of the body) is their bi-

directionality. This phenomenon is likely because the lung parenchyma encircles the blood

vessels from all sides so that regardless of the relative beam direction, the closer borders

move towards the beam source while those at the far side move away from it. As a result,

similar signals of opposite polarity are generated. In some cases, as depicted in FIG. 2 the

signals seem almost perfectly symmetrical. Such symmetry is rarely seen in non-pulmonary

records of blood flow.

[0047]   It is notable that with conventional Doppler measurements of blood flow

through vessels, where the movement is the blood flow itself, the probes are positioned so the

ultrasound beam is as parallel as possible to the flow axis to obtain maximal velocity. In

contrast, the motion that gives rise to the TPD measurements described herein is

perpendicular to the direction of blood flow, so the optimal position is normal to the flow axis

and parallel to the vessel radius. But since there are so many blood vessels in the lungs,

positioning is less critical in the context of TPD (as compared to conventional Doppler

measurements of blood flow through vessels).

[0048]   Since the features in FIG. 2 always have a repetition cycle corresponding to

the R-R interval of the ECG 24, we have concluded that they must originate from structures

that reflect ultrasound energy while moving in synchrony with the heart beat. These entities

could be the heart itself, the blood flowing in the pulmonary blood vessels, the pulsating

blood vessels, or their junctions with alveoli, alveolar sacs, air, etc.

[0049]   The recorded signals will be referred to as – Lung Doppler Velocity Signals,

(LDVS). FIG. 5A compares a typical LDVS 52 of a normal subject with tracings 55, 56 of

blood flow velocity in both a pulmonary artery and vein, for a single cardiac cycle, with the

cardiac cycle durations normalized to the same time scale (note the R-waves 26 of the ECG

24). Significant correlation is present. FIGS. 5B-E compare the LDVS 56 of normal

breathing (FIG. 5B) with those recorded during various respiratory maneuvers over a number

of cardiac cycles. For example, during breath-holding at FRC (functional residual capacity)

(FIG. 5C), the features 57 have normal shape and velocity but attenuated intensity. During a

Valsalva maneuver (FIG. 5D) in which the chest cavity pressure is greatly elevated, the

features 58 are seen to virtually disappear. In contrast, during a Muller maneuver (FIG. 5E),

which generates negative pressure within the chest cavity, both the velocity and signal power

of the LDVS 59 increase.

[0050]   The synchronization of the five features (#1-5) with the heart beat and

associated mechanical events indicates that the signal source is related to pulsations generated

by the heart and blood vessels, and the strong modulation of the features by respiratory

maneuvers (see FIGS. 5C-E) indicates that the state of the lung parenchyma strongly affects

their shape. The fact that similar signals are recorded throughout the lungs, in spite of the

strong mechanical dumping properties of the lung parenchyma, rules out direct involvement

of the heart and large blood vessels. Thus, it is most likely that the spread of the pulsations is

by propagation along the blood vessels in the lungs, including the relatively small ones.

[0051]   Based on the theory of operation set forth above, we interpret the five features

depicted in FIGS. 2 and 3 as follows: Feature #1, which is usually very prominent, appears

shortly after the R wave, and coincides with the systolic ventricular contraction. Feature #2,

which has lower peak velocity, coincides with the T wave of the ECG and repolarization and

ventricular relaxation. Feature # 3, which is often double humped and is of relatively longer

duration, seems to appear mainly during the diastolic rapid filling phase. Feature # 4, which

typically has a low peak velocity, corresponds to the diastasis, the latter part of which is often

not associated with a detectable signal. Feature # 5, which is usually of high peak velocity, coincides with atrial contraction.

[0052]   The relative amplitudes, rise times and fall times, durations etc. of these five features thus provide information regarding the blood flow hemodynamics, passive mechanical properties of the various cardio-vascular system components, as well as the active (contraction) forces. In addition, the displays provide information related primarily to the pulmonary system.

[0053]   To verify the theory that the returns are generated by a moving tissue-air boundary, a Doppler sonogram was made using a phantom where pseudo-blood (Doppler test fluid 707, ATS Laboratories Inc. CT, USA) incorporating miniature air bubbles (under 0.5mm) was flowing in an appropriate vessel. In the sonogram the bubbles appear as bright "blips". The power spectra of the flowing pseudo blood and bubbles reveal that the peak power generated by the moving air bubbles is about 40 dB higher than that of flowing pseudo-blood and coronary flow recorded under similar conditions. These results are compatible with the theory set forth above.

[0054]   Measurements were taken on 10 normal volunteers aged 27 – 72 over the right or left lung by means of an ultrasound sensor positioned over the chest wall of a sitting or supine subject. A 21 mm, 2 MHz sensor having a focal length of 4 cm was impedance matched with the chest wall by standard ultrasound gel. Measurements were made from different positions over the chest wall using a pulsed TCD device (Sonara/tek, Viasys, Madison, WI, USA) at a pulse repetition rate (PRF) of 3 kHz. The transmitted pulse power was up to 10% of the allowed maximal ISPTA.3 (492 mW/cm^2). The subjects were

17

connected to a standard three lead ECG (Norav Medical Ltd, Yokneam, Israel) the output of which was included in the display.

[0055]   Observing the resulting velocity-and-power vs. time traces can provide diagnostic information on the mechanical properties of the pulmonary parenchyma, in general and at specific locations when those traces deviate from the expected normal traces. This may include information related to the tissue structure (which may be relevant to emphysema, fibrosis, atelectasis, etc.), vasculature, or the presence of fluid in or around the alveoli (as in congestive heart failure or pneumonia, vascular events such as emboli & hemorrhage), etc. These deviations from normal can result from changes in the elastic properties as well as the mass of the various tissue elements as well as their spatial distribution. Such changes will result in global or local corresponding changes in the power spectra profiles, time constants, durations, or amplitudes (relative or absolute) of the traces. Physiological manipulations such as deep inspiration, forced expiration, breathe holding, Valsalva maneuvers, exercise, etc. may be used to enhance the diagnostic capabilities. Note that the ultrasound waves reflected from any intra-pulmonary element are modified as they pass through the lung parenchyma that intervenes between them and the chest wall. This tissue acts as a mechanical filter of specific characteristics. These characteristics depend on the state of the relevant parenchyma, such that the power spectra of the signals that pass through this filter reflect on the filter characteristics for acoustic signals as described by Gavriely N., Y. Palti & G. Elroy (Spectral Characteristics of Normal Breath Sounds, J. Appl. Physiol. 50: 307-314 (1981), which is incorporated herein by reference).

[0056]   Optionally, the signals from a single subject may be averaged over a number of cardiac cycles using the R wave 26 of the ECG 24 as a reference point. FIG. 6, for example, depicts an average 62 of ten cardiac cycles from a normal subject, recorded over the

right lung. Five features #61-65 can be seen, corresponding to features #1-5 discussed above. The traces were generally similar for other normal subjects.

[0057]   DETECTION AND CHARACTERIZATION OF CARDIAC FUNCTION

[0058]   One useful application of the TPD system described herein is as a tool for indirectly ascertaining the function of the cardiac system through TPD measurements of the lungs. This is possible because the outcome of the cardiac activities propagate along the pulmonary blood vessels from their origin in the heart to the whole lung volume. A number of clinically significant deviations from normal mechanical cardiac activity can be detected and characterized using TPD in this way, and some examples are given below.

[0059]   FIG. 7A depicts the changes from the normal pattern of lung signals in cases of arrhythmia due to atrial extra-systoles, which is a type of additional abnormal cardiac contraction. The left side of FIG. 7A depicts signals typical of a normal sinus rhythm, and the right side depicts the appearance of an atrial extra-systole 71 (i.e., the signals generated by an early electrical beat produced by the sinus node) that propagates to the ventricles. These signals are basically a duplicate of the normal rhythm complex, i.e. they include and extra atrial contraction (feature #5) followed by an extra ventricle contraction (feature #1) and ventricle relaxation (feature #3). When they occur early enough, the atrial contraction signal (feature #5) may superpose in time over previous ventricular relaxation (feature #3). FIG. 7B illustrates the characteristics of a signal produced by an atrial extra-systole 73 resulting in an atrial contraction (feature #5) that does not propagate from the atrium to the ventricles, as manifested by the absence of features # 1 and #3 after the abnormal additional feature #5*.

19

[0060]   FIG. 8 illustrates signals produced by Extra-Systolic contractions (feature #1*)

generated by electric abnormal activity 82 in the ventricle. FIG. 9 depicts signals

corresponding to contractions of ventricular origin (#1) in a patient suffering from atrial

fibrillation. This condition is apparent from FIG. 9 because feature #5 (representing atrial

contraction) is missing. It is also seen that the characteristics of the ventricular extra-systoles

are very different from those of the atrial extra-systoles, reflecting the large differences of the

nature of the mechanical activity. Such recorded tracings can help the physician determine

the pathway of propagation of the abnormal activity.

[0061]   The presence of any of the abnormal features discussed above in connection

with FIGS. 7A, 7B, 8, and 9, can therefore be used as an indication that the patient has the

corresponding problem. This may be accomplished visually, by looking at the displays and

recognizing the relevant features. In alternative embodiments, pattern recognition software

may be used to recognize the relevant features automatically.

[0062]   MULTI-POSITION MEASUREMENTS

[0063]   TPD measurements may be taken from different lung depths, and such

measurements usually show very similar tracings indicating a wide spread of the signals in

the lung volume. Measurements may also be taken from different positions on the subjects'

body, such as over the intercostal spaces (e.g. between the 2nd and 3rd ribs or between the

5th and 6th ribs) as well as from positions over the ribs. When such measurements are taken

at multiple positions, in some cases there are significant differences between the signal

shapes, velocities, and power measurements taken at each position. The inventors have

recognized that such recordings in general and specifically recording differences may be used

to help diagnose certain physiological conditions.

[0064]   In one example, measurements were made on two chronic obstructive

pulmonary disease (COPD) patients' right lungs at three different positions locations over

each patient's right lung: an upper zone at the level of the 2-3 ribs, a middle zone at the level

of the 4th rib, and a lower zone at the level of the 5-6 ribs. Unlike the normal subjects in

which the measurements taken at the upper, middle, and lower positions were very similar, in

the COPD patients the signals at the upper zone were significantly smaller than those in the

middle zone, which were in turn significantly smaller than the signals at the lower zone. In

addition, the signal shapes (e.g., the degree of symmetry in velocity and power) were also

different in the different zones. This deviation from the normal situation can be used as

predictor for the presence of COPD. Similarly, other deviations from the normal situation

can be used as predictor for the presence of other abnormal conditions.

[0065]   The average peak positive and negative velocities for features #1, 3, and 5

were measured for a group of patients (including normal patients, COPD patients, sarcoidosis

patients, and a fibrosis patient) from each of those three positions (i.e., upper, middle, and

lower). That experimental data is depicted in FIGS. 10A-C, with positive and negative

velocities on the y-axis. The normal patients are the ones on the left, the patients between FS

and DUL had COPD, the patients between BAD and BUJ had sarcoidosis, and the patients

between RL and EHOE had fibrosis. In FIG. 10A, each group of 3 Bars (left, center, and

right) represents the results of the average peak positive and negative velocity (in cm/sec) that

was obtained for feature #1 in the upper, middle, and lower zones, respectively, for each

patient. FIGS. 10B and 10C depict corresponding data for features # 3 and 5. Note that the

labels U, M, and L (which denote the upper, middle, and lower zones, respectively) have only

been included for one patient in each of FIGS. 10A-C to avoid clutter.

[0066]   Examination of the data depicted in FIGS. 10A-C reveals that in normal

patients, the velocities for feature #1 were roughly similar in all three zones. But in the

COPD patients, the velocity was much lower in the upper zone than in the middle zone, and

the velocity was much lower in the middle zone than in the lower zone. The same situation

was true for feature #5. The presence of those relative velocities for features #1 and 5 can

therefore be used as a predictor for the presence of COPD. The test for distinguishing

between normal and COPD patients may be fixed (e.g., COPD may be indicated if the peak

velocity of the middle reading is at least twice as large as the peak velocity of the upper

reading and the peak velocity of the lower reading is at least three times as large as the peak

velocity of the upper reading). Alternatively, the threshold levels may be obtained using

parameterization as described below. Thus, we see that the differences between the velocities

for the features at different locations can be used to help distinguish between normal subjects

and patients with various diseases.

[0067]   FIG. 11A is a graphical representation of the differences between normal and

COPD subjects, based on the averages of those two groups of patients, which highlights the

distinction between the peak velocities for features #1 and #5 at the upper, middle, and lower

zones.

[0068]   Optionally, the above described data may be combined with "power

sonogram" data, as described in US application 12/771,091, filed April 30, 2010, which is

incorporated herein by reference. The personal computer 13 (show in FIG.1) should then be

programmed to extract the power data from the ultrasound returns as described in the '091

application. FIG. 11B demonstrates that power data so obtained can serve to differentiate

between normal subjects, patients with COPD, and patients suffering from pulmonary

fibrosis. In the latter, connective tissue that conducts ultrasound energy well replaces the air

22

filled alveoli and thus one obtains higher total power values. Note also that in the case of

fibrosis (in contrast to the normal and COPD cases) the largest power signal is often recorded

from the upper lung segment. This may be used as a predictor for the presence of fibrosis.

[0069]   Distinctions between the Congestive Heart Failure (CHF), pulmonary

emphysema, and edemas can also be characterized by differences their Doppler signatures.

For example, in edema patients the power will be lower than normal, but in CHF patients the

power may be higher than normal due to the excess fluid in the lungs (which provides less

signal attenuation that the air that would ordinarily be there in a normal patient). The power

distribution between the different lung zones may be altered with the local changes in the

lung parenchyma and vasculature. These distinctions may be detected using TPD and relied

on to diagnose those conditions, either visually from the displayed power-and-velocity vs.

time displays, or automatically using appropriate pattern recognition or parameterization

software. Similar concepts may be used for other pathologies.

[0070]   AUTOMATIC FEATURE RECOGNITION

[0071]   The discussion above makes frequent references to features #1-5. Optionally,

software that recognized the delineation between each of those features may be implemented

in the personal computer 13 (shown in FIG. 1). Automatic feature recognition ("AFR") may

be implemented on the averaged signals discussed above in connection with FIG. 6, on a

single signal (e.g., as depicted in FIG. 2), or after the averaging operation contained within

the NR (i.e., the first phase of the noise reduction routine discussed above). FIG. 12 is an

example of automatic feature recognition based on the latter. In FIG. 12, each of the features

#1-5 is bounded by two local minimum points on the calculated envelope, and defined

according to the relative location of its peak velocity (i.e., maximum point) and the averaged

signals' ECG waveforms. These local minima define the transitions 181-185 between the various features and are denoted by dashed lines in FIG. 12. In a regular cardiac rhythm, the features are defined in relation to the ECG signal 24 as follows: #1 – the segment with the first velocity peak after the first R-wave 26; #2 – the segment with the first velocity peak after feature #1 but preceding the ECG's T-wave; #3 – the segment with the first velocity peak after the T-wave ends; #4 – the segment bounded between feature #3 and feature #5; and #5 – the segment with the velocity peak that immediately precedes the next R wave and next feature #1.

[0072]   AFR can be useful because the absolute and relative calculated parameters that characterize these segments may be used to classify and diagnose a pathology and its location. These parameters are useful for automated recognition of various conditions that rely on parameterization, discussed below.

[0073]   PARAMATERIZATION

[0074]   Parameterization may be used to characterize the various features so as to diagnose and estimate the extent of various pathologies such as COPD, Sarcoidosis, Fibrosis asthma, emphysema, pulmonary hypertension, pulmonary embolism, tumors, arteriosclerosis of pulmonary vessels, atelectasis, cardiac contractile dysfunction, and arrhythmia etc. Quantification of the various parameters may be done on specific segments and the relations between them, as well as on the variability of the signals in the original spectrogram (i.e., before it was averaged). The parameterization may be implemented using the approaches described in US application 12/700,828 ("the '828 application"), filed February 5, 2010, which is incorporated herein by reference.

24

[0075]   Some of the data is derived from the power spectra themselves as provided by the Doppler measurements. The features of these power spectra may also be parameterized, for example the power at specific velocities, the average slopes of the curves, the number of different slopes at the positive and negative features etc. Parameters may also be derived from the velocity and power versus time tracings. The tables below contain examples of parameters that may be used to parameterize the TPD results, and their definitions:

Velocity Features:
$peak\_velocity\{PDS_i\} = \max(envelope\{PDS_i\})$
$peak\_velocity\_ratio\{PDS_{i,j}\} = \frac{peak\_velocity\{PDS_i\}}{peak\_velocity\{PDS_j\}}$
$max\_slope\{PDS_i\} = \max\{\frac{d}{dt}(envelope\{PDS_i\})\}$
$VTI\{PDS_i\} = \Delta t \cdot \sum_{PDS_i} envelope\{PDS_i\}$
$ADPV\{PDS_i\} = \frac{1}{t2-t1+1} \sum_{PDS_i=t1}^{t2} envelope\{PDS_i\}$
$std\_peak\_velocity\{PDS_i\} = std(peak\_velocity\{PDS_{orig\_i}\})$ $(PDS_{orig\_i}) \in cycles\_before\_averaging$
$Mean\_weighted\_V = \dfrac{\sum\limits_{t=t1}^{t2} \sum\limits_{v=0}^{envelope_{(t)}} (P_{(t,v)} \cdot v)}{\sum\limits_{t=t1}^{t2} \sum\limits_{v=0}^{envelope_{(t)}} P_{(t,v)}}$
$MMWVC = \dfrac{\Delta t \cdot \sum\limits_{t=t1}^{t2} \left(\dfrac{\sum\limits_{v=0}^{envelope_{(t)}} (P_{(t,v)} \cdot v)}{\sum\limits_{v=0}^{envelope_{(t)}} P_{(t,v)}} \right)}{t2-t1+1}$

Power Features:
$Mean\_power = mean\{P_{(t,v)}\}_{(t,v) \in PDS\_i}$
$Max\_power = \max\{P_{(t,v)}\}_{(t,v) \in PDS\_i}$
$Median\_power = median\{P_{(t,v)}\}_{(t,v) \in PDS\_i}$

$$std\_power\_flow = std \left\{ P_{(t,v)} \right\}_{(t,v) \in PDS\_i}$$

$$std\_power\_flow\_dB = std \left\{ 10 \cdot \log_{10} \left(P_{(t,v)} + 1 \right) \right\}_{(t,v) \in PDS\_i}$$

$$PVTI = \Delta v \cdot \Delta t \cdot \sum_{t=t1}^{t2} \sum_{v=0}^{envelope_{(t)}} \left(P_{(t,v)} \cdot v \right)$$

$$total\_power = \Delta v \cdot \Delta t \cdot \sum_{t=t1}^{t2} \sum_{v=0}^{envelope_{(t)}} P_{(t,v)}$$

Time Features:
$PDS\_duration = \left\{ t_{end} - t_{start} \right\}_{(t) \in PDS\_i}$
$PDS\_ECG\_syncronization = abs \left(t(\max\_velocity \{ PDS_i \}) - t(\max(R/T - wave))) \right)_{(t,v) \in ROI}$
$duration\_percentage = \left(\dfrac{PDS\_duration}{\left(t_{end} - t_{start} \right)_{(t) \in averaged\_cycle}} \right)_{(t,v) \in ROI}$

Other Features
Age
Weight
Sex
Height

[0076]   Using these parameters, the learning and classifying steps may be implemented as described in the '828 application.

[0077]   CONCLUSION

[0078]   The Doppler signatures of the following of tissues and structures may change with pathology: pulmonary emphysema, pulmonary emboli, pulmonary hypertension, pulmonary blood vessel stenosis & malformations, conditions associated with pulmonary fibrosis, pneumonia, atelectasis, pneumothorax, congestive heart failure, pulmonary solid tumors, various cardiac malfunctions that are manifested in the pulmonary blood vessels, tumors, and foreign bodies, etc. Thus, the lung Doppler signals picked up using TPD may be used to provide insights and potentially valuable diagnostic information regarding the structure and integrity of the lung parenchyma and vasculature. TPD may therefore serve as a new non-invasive and non-destructive tool for diagnosis of pulmonary disease & function.

26

It may also enable continuous monitoring of the status of a failing pulmonary or cardio-

vascular system, and help determine the efficacy and so enable dose calibration, for optimal

treatment.

[0079]   An additional unique diagnostic capability of the TPD is to determine the

compliance (elastance) of the pulmonary vascular tree components that changes in cases of

arteriosclerosis and other vascular conditions. Vascular compliance can be measured on the

basis of the pulse propagation velocity in the vessel because the more rigid the vessel is, the

faster the propagation will be. In the case of the lungs, the propagation velocity can be

determined from the delay between the time of appearance of any of the lung signals (or their

peak, etc.), at different locations along the propagation pathway. Such delay measurements

can be made, manually or automatically by appropriate software, in the different records

obtained at different lung locations or at different depths beneath a single location.

[0080]   While the present invention has been disclosed with reference to certain

embodiments, numerous modifications, alterations, and changes to the described

embodiments are possible without departing from the sphere and scope of the present

invention, as defined in the appended claims. Accordingly, it is intended that the present

invention not be limited to the described embodiments, but that it has the full scope defined

by the language of the following claims, and equivalents thereof.

27

WHAT IS CLAIMED IS:

1.   A method of evaluating the functionality of a patient's heart or lungs, the method comprising the steps of:

transmitting ultrasound energy into the patient's lung;

detecting Doppler shifts of reflected ultrasound induced by moving borders between blood vessels in the lung and air filled alveoli that surround the blood vessels, wherein movement of the border is caused by pressure waves in the blood vessels that result in changes in diameter of those blood vessels;

processing the detected Doppler shifts with an algorithm designed to increase signal from the moving border with respect to other reflected ultrasound signals and outputting processed power and velocity data; and

displaying the outputted power and velocity data.

2.   The method of claim 1, further comprising the step of diagnosing a condition of the patient's heart based on a result of the displaying step.

3.   The method of claim 1, further comprising the step of diagnosing a condition of the patient's lung based on a result of the displaying step.

4.   The method of claim 1, further comprising the step of displaying an ECG that is aligned in time with the data displayed in the displaying step, using a common time scale.

5.   The method of claim 1, wherein the transmitting step comprises transmitting an ultrasound beam with an effective cross section of at least ½ cm.

6.   The method of claim 1, wherein the processing step involves an algorithm that

comprises the steps of:

(a) calculating P(t) = {mean of A(t) in noise region} for each time t = {1,2, ... N};

(b) defining a threshold 'thr2' based on the average and std of {P(1),P(2),... P(N)}; and

(c) reducing P(t') by raising an upper envelope or lowering a lower envelope until P(t')<=thr2,

for each t' where P(t')>thr2.

7.   The method of claim 6, wherein the processing step implements a Chan-Vese

algorithm.

8.   A method of evaluating the functionality of a patient's heart or lungs, the method

comprising the steps of:

        obtaining, using an ultrasound probe that is aimed at the patient's lung, Doppler

ultrasound power and velocity data for a period of time that corresponds to at least one

cardiac cycle;

        processing the power and velocity data obtained in the obtaining step using at least

one noise reduction algorithm;

        displaying, on a display, the processed power and velocity data for the period of time;

and

        correlating an abnormality in at least one of (a) a feature on the display that

corresponds to systolic ventricular contraction, (b) a feature on the display that corresponds to

ventricular relaxation, (c) a feature on the display that corresponds to a diastolic rapid filling

phase, (d) a feature on the display that corresponds to diastasis, and (e) a feature on the

29

display that corresponds to atrial contraction with an abnormal condition of the patient's heart or lungs.

9.   The method of claim 8, wherein the abnormality is that at least one of the features is absent or has an unexpected shape.

10.   The method of claim 8, wherein the abnormality is that an unexpected additional feature is present.

11.   The method of claim 8, wherein the abnormality is that at least one of the features occurs at an incorrect time.

12.   The method of claim 8, further comprising the step of displaying an ECG that is aligned in time with the data displayed in the displaying step, using a common time scale.

13.   The method of claim 8, wherein the obtaining step comprises generating an ultrasound beam with an effective cross section of at least ½ cm.

14.   The method of claim 8, wherein the at least one noise reduction algorithm comprises the steps of:

(a) calculating $P(t) = \{$mean of $A(t)$ in noise region$\}$ for each time $t = \{1,2, \ldots N\}$;

(b) defining a threshold 'thr2' based on the average and std of $\{P(1),P(2),\ldots P(N)\}$; and

(c) reducing $P(t')$ by raising an upper envelope or lowering a lower envelope until $P(t') <= thr2$, for each t' where $P(t') > thr2$.

30

15.   The method of claim 14, wherein the at least one noise reduction algorithm further comprises the step of implementing a Chan-Vese algorithm.

16.   The method of claim 8, further comprising the step of averaging the ultrasound power and velocity data for a plurality of cardiac cycles, wherein the averaging step is performed prior to the displaying step.

17.   A method of evaluating the functionality of a patient's heart or lungs, the method comprising the steps of:

        obtaining, using an ultrasound probe that is aimed at the patient's lung, Doppler ultrasound power and velocity data for a period of time that corresponds to at least one cardiac cycle;

        processing the power and velocity data obtained in the obtaining step using at least one noise reduction algorithm;

        checking for abnormalities in (a) a feature of the processed power and velocity data that corresponds to systolic ventricular contraction, (b) a feature of the processed power and velocity data that corresponds to ventricular relaxation, (c) a feature of the processed power and velocity data that corresponds to a diastolic rapid filling phase, (d) a feature of the processed power and velocity data that corresponds to diastasis, and (e) a feature of the processed power and velocity data that corresponds to atrial contraction; and

        correlating an absence of abnormalities in the checking step with a normal condition of the patient's heart or lungs.

18.   The method of claim 17, further comprising the step of displaying, on a display, the processed power and velocity data for the period of time, and wherein the checking step is performed by a human by observing the display.

19.   The method of claim 18, further comprising the step of displaying an ECG that is aligned in time with the data displayed in the displaying step, using a common time scale.

20.   The method of claim 17, wherein the obtaining step comprises generating an ultrasound beam with an effective cross section of at least ½ cm.

21.   The method of claim 17, wherein the at least one noise reduction algorithm comprises the steps of:

(a) calculating P(t) = {mean of A(t) in noise region} for each time t = {1,2, ... N};

(b) defining a threshold 'thr2' based on the average and std of {P(1),P(2),... P(N)}; and

(c) reducing P(t') by raising an upper envelope or lowering a lower envelope until P(t')<=thr2, for each t' where P(t')>thr2.

22.   The method of claim 21, wherein the at least one noise reduction algorithm further comprises the step of implementing a Chan-Vese algorithm.

23.   The method of claim 17, further comprising the step of averaging the ultrasound power and velocity data for a plurality of cardiac cycles, wherein the averaging step is performed prior to the displaying step.

32

24.   A method of evaluating the functionality of a patient's heart or lungs, the method

comprising the steps of:

obtaining, using an ultrasound probe that is aimed at a first position of the patient's

lungs, a first set of Doppler ultrasound power and velocity data for a period of time that

corresponds to at least one cardiac cycle;

obtaining, using an ultrasound probe that is aimed at a second position of the patient's

lungs, a second set of Doppler ultrasound power and velocity data for a period of time that

corresponds to the at least one cardiac cycle;

generating a first output by processing the first set of data using at least one noise

reduction algorithm; and

generating a second output by processing the second set of data using at least one

noise reduction algorithm.

25.   The method of claim 24, further comprising the step of comparing the first output and

the second output.

26.   The method of claim 25, further comprising the step of correlating a result of the

comparing step with a presence of an abnormality in the patient's heart or lungs.

27.   The method of claim 25, further comprising the step of correlating a result of the

comparing step with an absence of an abnormality in the patient's heart or lungs.

28.   The method of claim 24, further comprising the steps of:

obtaining, using an ultrasound probe that is aimed at a third position of the patient's

lungs, a third set of Doppler ultrasound power and velocity data for a period of time that

corresponds to the at least one cardiac cycle, wherein the first position is higher on the

patient's body than the second position and the second position is higher on the patient's

body than the third position;

generating a third output by processing the first set of data using at least one noise

reduction algorithm; and

correlating a situation in which (a) peak velocity components of the third set of data

are significantly larger than peak velocity components in the second set of data and (b) peak

velocity components of the second set of data are significantly larger than peak velocity

components in the first set of data with the presence of COPD.
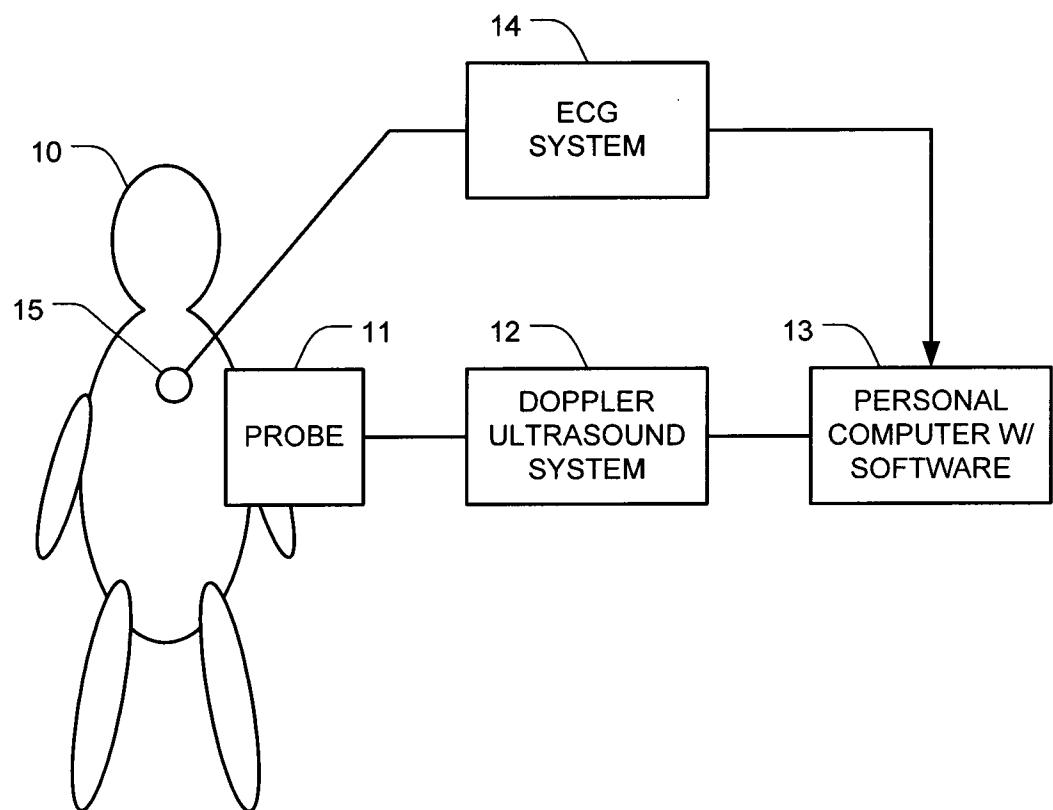
FIG. 1
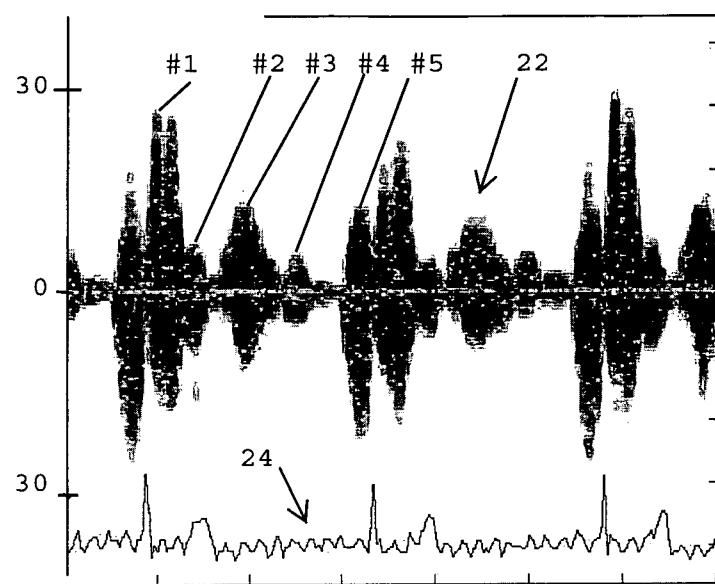
FIG. 2
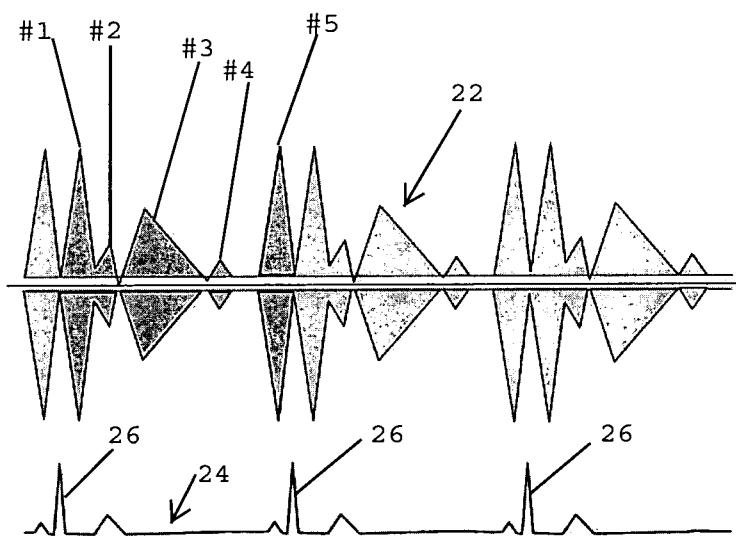
FIG. 3
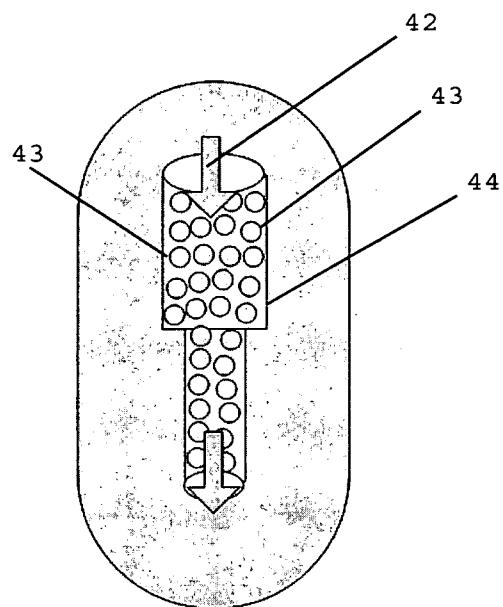
FIG. 4A
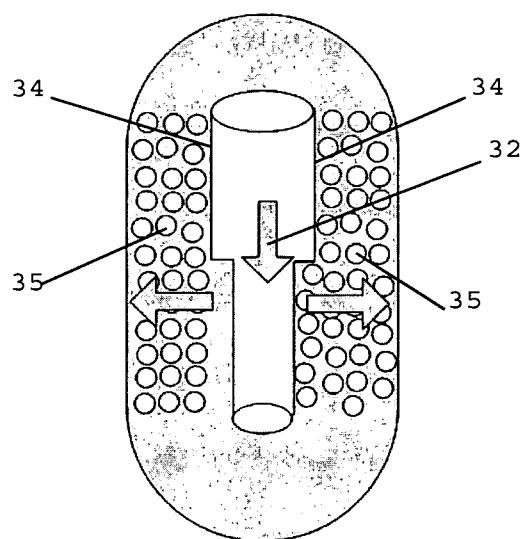
FIG. 4B
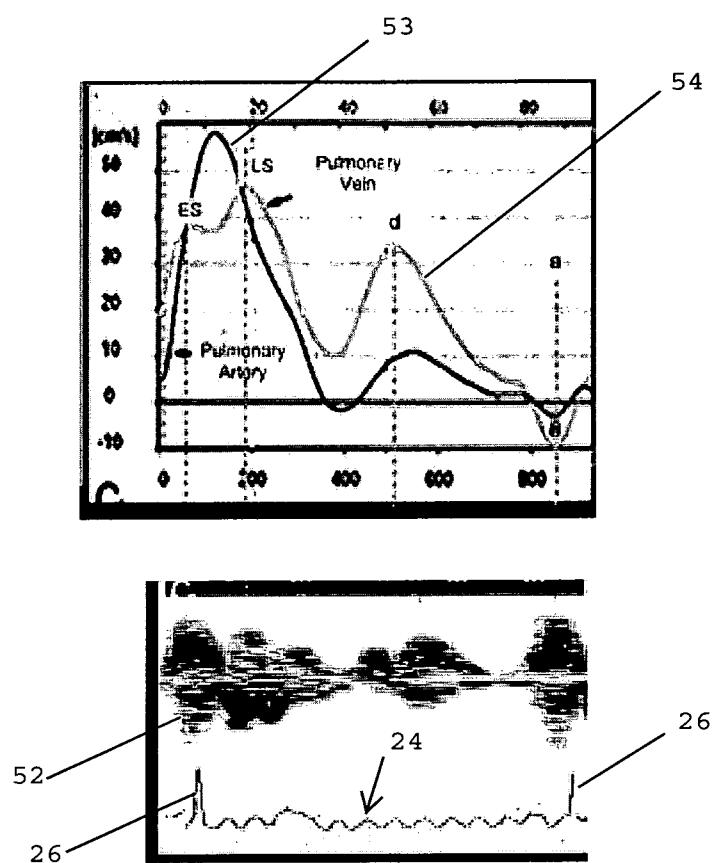
FIG. 5A
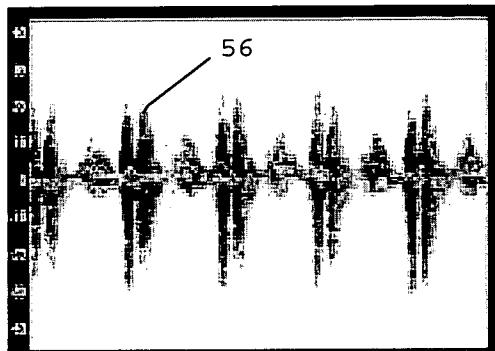
FIG. 5B
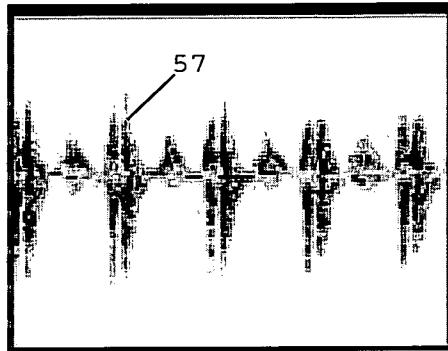
FIG. 5C
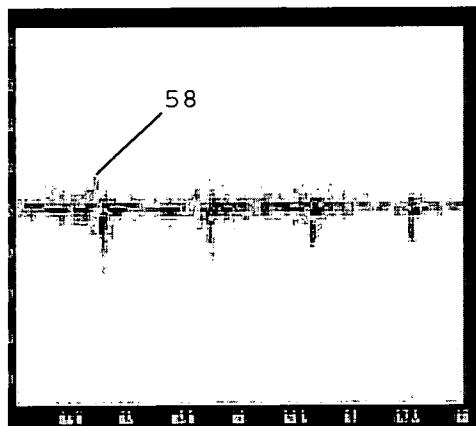
FIG. 5D
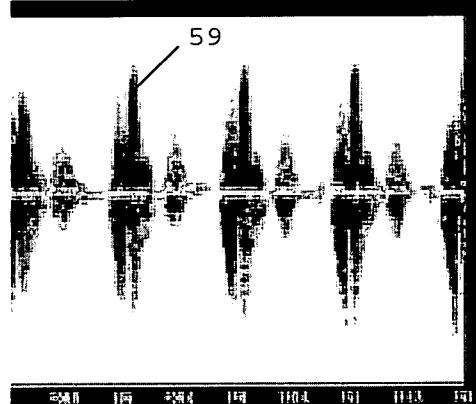
FIG. 5E
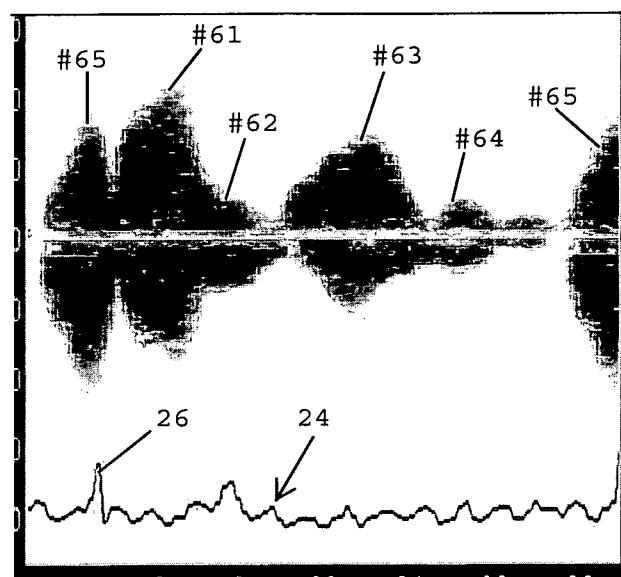
FIG. 6
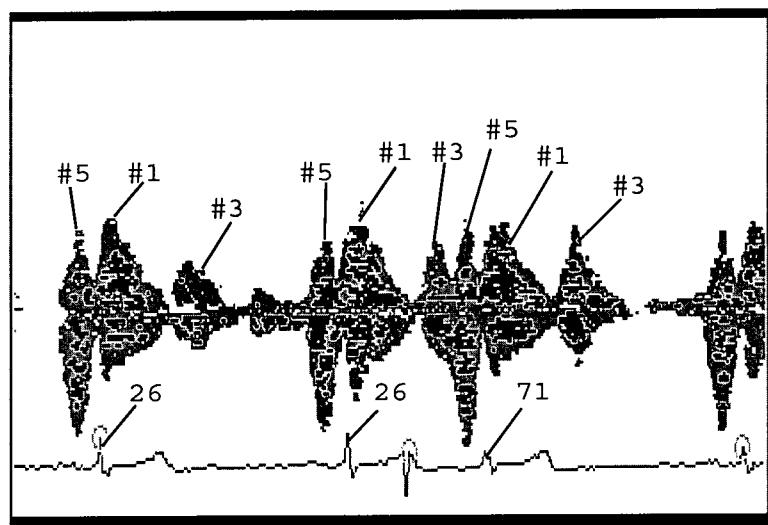
FIG. 7A
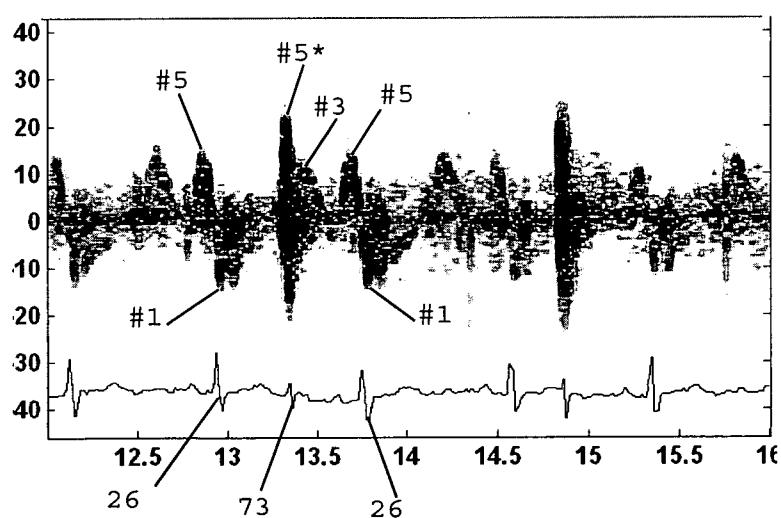
FIG. 7B
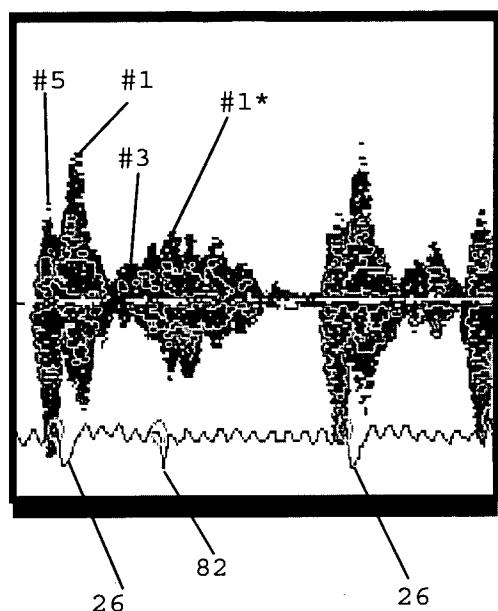
FIG. 8
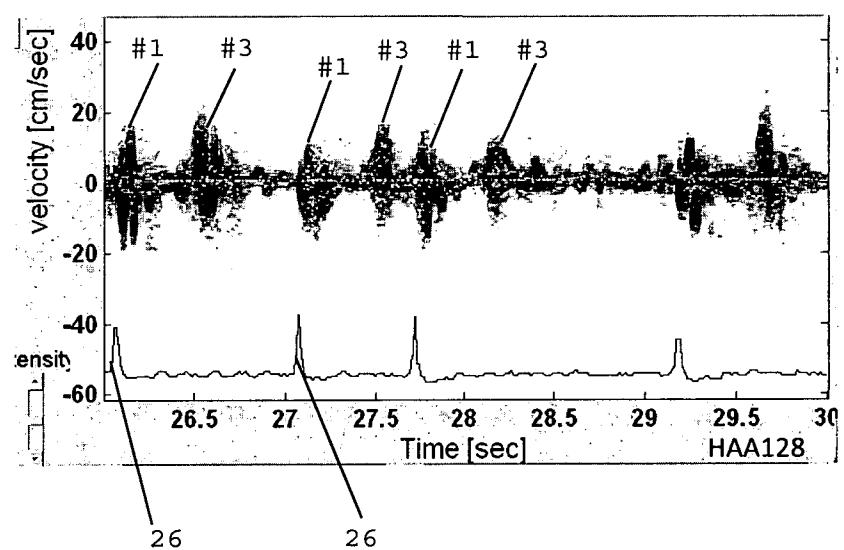
FIG. 9
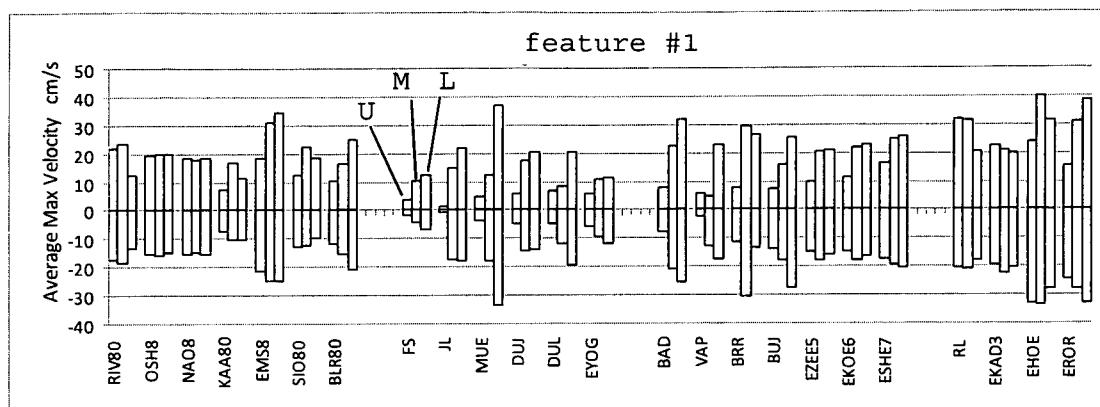
FIG. 10A

FIG. 10B

FIG. 10C

FEATURE #1

FEATURE #5
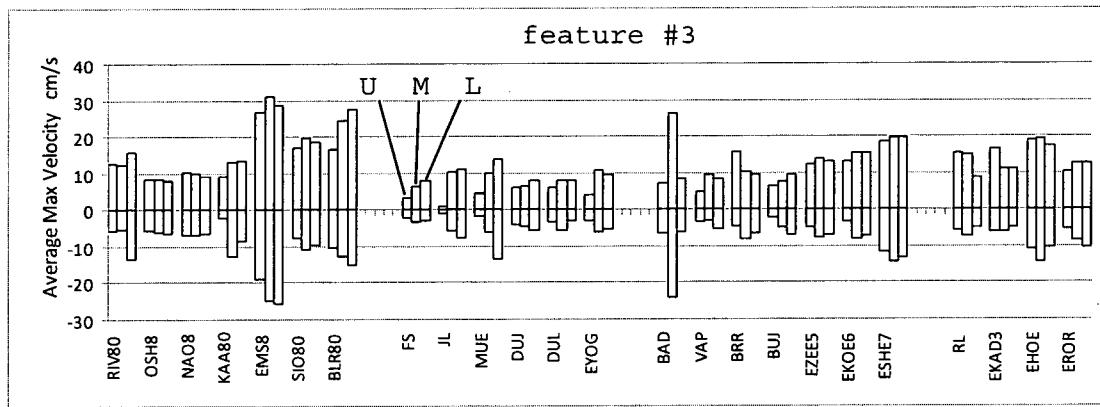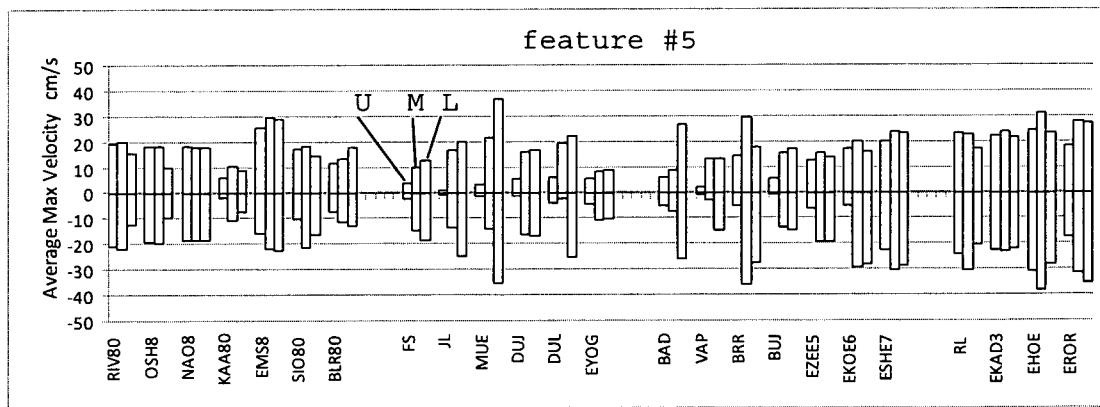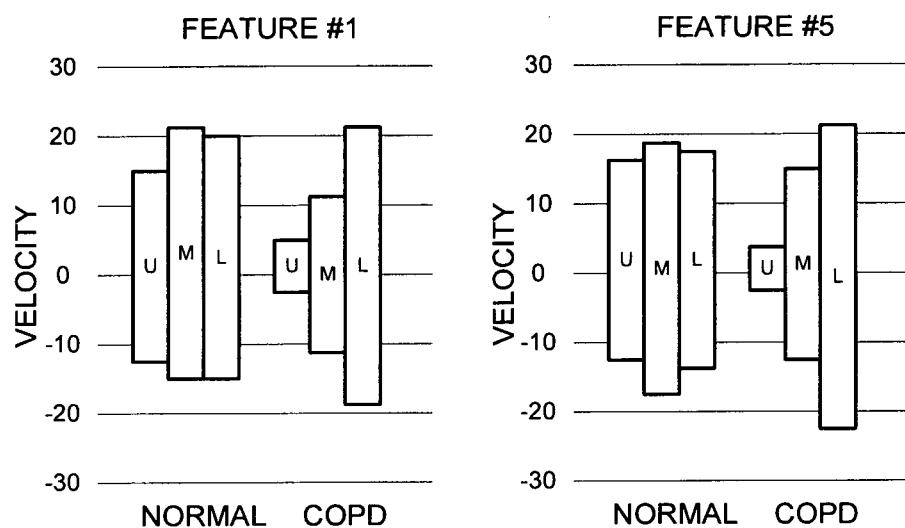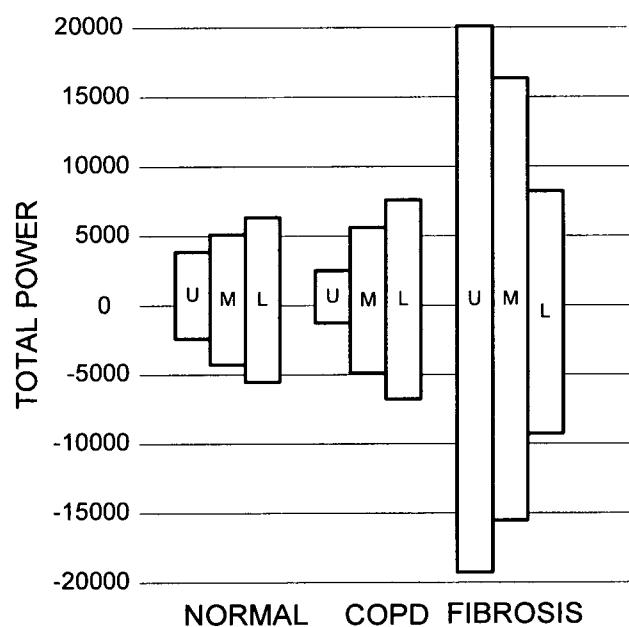
FIG. 11A

FIG. 11B
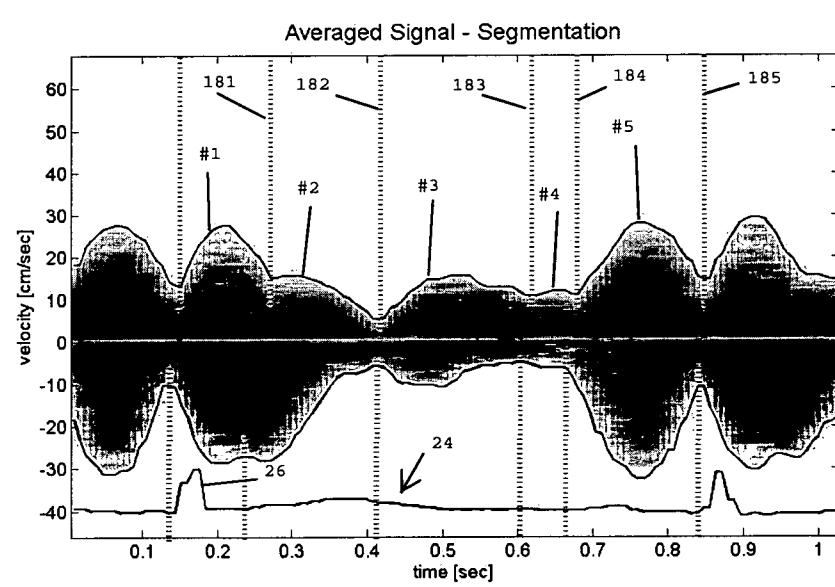
FIG. 12

专利名称(译)	经胸肺多普勒超声		
公开(公告)号	[EP2493386A2](#)	公开(公告)日	2012-09-05
申请号	EP2010784341	申请日	2010-10-27
[标]申请(专利权)人(译)	约拉姆帕提 的Lempel MEYTAL 坎特AYELET WASSERMAN约拉姆		
申请(专利权)人(译)	帕提，约拉姆 的Lempel，MEYTAL 坎特，AYELET WASSERMAN，约拉姆		
当前申请(专利权)人(译)	帕提，约拉姆 的Lempel，MEYTAL 坎特，AYELET WASSERMAN，约拉姆		
[标]发明人	PALTI YORAM LEMPEL MEYTAL KANTER AYELET WASSERMAN YORAM		
发明人	PALTI, YORAM LEMPEL, MEYTAL KANTER, AYELET WASSERMAN, YORAM		
IPC分类号	A61B8/08		
CPC分类号	A61B8/02 A61B8/06 A61B8/08 A61B8/0883 A61B8/488 A61B8/5223 A61B8/543 G16H50/30 A61B5/0205 A61B5/044 A61B5/08 A61B8/04 A61B8/463 A61B8/5269 A61B8/5284		
代理机构(译)	博登KEITH麦克默里		
优先权	61/255322 2009-10-27 US 61/326133 2010-04-20 US 61/405454 2010-10-21 US		
外部链接	[Espacenet](#)		

摘要(译)

可以通过将超声能量发射到患者的肺中来检测患者的心脏或肺的操作，并且检测由肺中的血管和围绕血管的充满空气的肺泡之间的边界移动引起的反射超声的多普勒频移。边界的移动是由血管中的压力波引起的，这些压力波导致那些血管的直径变化。利用算法处理检测到的多普勒频移，该算法被设计成相对于其他反射的超声信号增加来自移动边界的信号，然后显示结果。